Journal of Power Sources 253 (2014) 41–47

Contents lists available at ScienceDirect

Journal of Power Sources

journal homepage: www.elsevier.com/locate/jpowsour

Novel photoelectrochemical behaviors of p-SiC films on Si for solar water splitting

Quan-Bao Ma [a,b,*], Bernhard Kaiser [a], Wolfram Jaegermann [a]

[a] Department of Materials Science and Center of Smart Interfaces, Technische Universität Darmstadt, Petersenstraße 32, D-64287 Darmstadt, Germany
[b] Department of Chemical Engineering and Chemistry, Eindhoven University of Technology, 5600 MB Eindhoven, The Netherlands

HIGHLIGHTS

- p-SiC film on p-Si substrate as a photocathode can generate appreciable cathodic photocurrent.
- p-SiC film on p-Si substrate as a photoanode also can generate weak anodic photocurrent.
- p-SiC film on n-Si substrate can only generate obvious anodic photocurrent.
- The dual photocurrent behaviors of p–p structure were investigated and proposed.
- No other groups reported such dual photocurrent behaviors of p–p structure.

ARTICLE INFO

Article history:
Received 21 October 2013
Received in revised form
2 December 2013
Accepted 9 December 2013
Available online 18 December 2013

Keywords:
SiC
Single crystalline
Photoelectrochemical properties
Photocurrent
Solar energy
Water splitting

ABSTRACT

The electrochemical properties of single-crystalline p-type 3C-SiC films on p-Si and n-Si substrates were investigated as electrodes in H_2SO_4 aqueous solutions in dark and under light illumination. The photoelectrochemical measurements with different wavelengths of light sources indicate the p-SiC film on p-Si substrate can generate a cathodic photocurrent as a photocathode, which corresponds to hydrogen production, and generate an anodic photocurrent as a photoanode, which corresponds to oxygen evolution. The photocurrent density on wavelength at different potentials for p-SiC on p-Si was investigated. IPCE measurements were addressed to study the photoactive wavelength regimes for the p-SiC film on p-Si and the p-Si. For p-SiC film on n-Si substrate, it can only generate an apparent photocurrent as a photoanode for oxygen evolution. The analyses on anodic and cathodic photocurrent behaviors of the p-SiC on p-Si and the p-SiC on n-Si as electrodes were proposed.

1. Introduction

Solar energy is the only renewable energy source with the hope to completely fulfilling the worldwide energy demands of our planet in the future since the consumption of fossil fuels is leading to pollution, harmful climate change, and eventual exhaustion of the carbon-based fuels. Today much attention has been paid to hydrogen as an alternative energy carrier to fossil fuels thanks to its non-toxic and environmentally friendly nature. The use of hydrogen promises to overcome energy and environmental issues, because it can be efficiently converted to electric and thermal energy by its consumption in a fuel cell, leaving only water as a by-product and no pollutants [1]. Since Fujishima and Honda [2] first demonstrated that water can be cleaved into its constituents at a chemically biased TiO_2 electrode with ultraviolet (UV) in a photoelectrochemical (PEC) cells in 1972, the PEC production of H_2 and O_2 using semiconductor photoelectrodes has received considerable attention [3,4]. Direct solar-driven photoelectrolysis of water has great potential to provide hydrogen for a sustainable and environmental hydrogen economy [5,6]. The generation of hydrogen by splitting water under solar illumination in PEC cells is of great interest as it offers an environmentally "green" approach to hydrogen production and has been considered for decades as a major enabling technology [7,8]. The efficiency of the process is largely determined by photosensitivity of the photoelectrode [9]. To explore an efficient and economical PEC process for renewable hydrogen production, significant efforts have been focused on the semiconductor materials [10,11].

* Corresponding author. Department of Materials Science and Center of Smart Interfaces, Technische Universität Darmstadt, Petersenstraße 32, D-64287 Darmstadt, Germany.
E-mail address: mqb7925921@163.com (Q.-B. Ma).

0378-7753/$ – see front matter © 2013 Elsevier B.V. All rights reserved.
http://dx.doi.org/10.1016/j.jpowsour.2013.12.042

For photoassisted water splitting, the principles of semiconductor physics must be combined with those of electrocatalysis. Direct photoelectrolysis systems require the semiconductor should simultaneously satisfy several material conditions relating to both the bulk and the interface with the electrolyte. First, the unassisted photoelectrolysis of water requires 1.23 V of photopotential from semiconductive materials which have band edges spanning both the oxidation and reduction potentials for the decomposition of water [12,13]. But considering the cathodic and anodic overpotentials, the minimum bandgap would be in the range of 1.6–1.9 eV [14]. However, for efficiently absorbing the solar spectrum and increasing the solar conversion efficiencies, the semiconductor bandgap should be less than 2.8 eV [15]. The second criterion requires that the minority band-edge potential and the bulk Fermi level potential encompass the half reactions of the electrolysis reactions of interest, that is for n-type semiconductor, the Fermi level should be higher than the hydrogen evolution (H_2/H_2O) redox potential and the valence band (VB) edge energy level should be lower than the oxygen evolution (H_2O/O_2) redox potential but for p-type semiconductor the conduction band (CB) edge energy level should be higher than the hydrogen evolution (H_2/H_2O) potential and the Fermi level should be lower than the oxygen evolution (H_2O/O_2) potential [16]. Besides, the semiconductor must be stable against photocorrosion in aqueous solutions.

Up to now, $GaInP_2$ [17,18], Cu_2O [19–22], InGaN [23,24], Fe_2O_3 [25] and SiC films [26–28], etc. have been used as photocathodes for solar water splitting. However, most of these films are grown on heterogeneous substrates, which form p–p structure or p–n structure. Therefore, it is not one layer but the multilayer that acts as the photocathode. Although the H_2 evolution photocurrents can be obtained by using multilayer structure as the photocathode but the photocurrent for H_2 evolution must be adapted to each other. So far these effects have hardly been considered and also no analysis on this phenomenon has been reported to our knowledge. From our studies on p-SiC on p-Si substrate and p-SiC on n-Si substrate as electrodes for solar water splitting, we have analyzed the photocurrent behaviors of such multilayer devices.

In this study the electrochemical (EC) properties of single-crystalline p-type 3C-SiC films on p-Si and n-Si substrates were investigated as electrodes in H_2SO_4 aqueous solutions in dark and under light illumination. The incident-photon-to-current-conversion efficiency (IPCE) measurements were addressed to study the photoactive wavelength regimes for the p-SiC film on p-Si and the p-Si. Besides, the analyses on the PEC behaviors of the p-SiC on p-Si substrate and the p-SiC on n-Si substrate as photoelectrodes were proposed.

2. Experimental section

Single-crystalline p-type 3C-SiC films on p-type Si and n-type Si substrates donated by the Leibniz Institute for Crystal Growth (IKZ), Berlin, were used. The thickness of SiC films is around 6 μm and the doping concentration was 10^{15}–10^{16} cm^{-3} characterized by secondary ion mass spectrometry. The surface was cleaned by acetone and isopropanol in ultrasonic bath. 100 nm gold was deposited on the etched backside as an ohmic contact. Before the EC measurements the surface of p-SiC was etched by HF solution (10 wt%) for 1–3 min to remove the oxide surface. The PEC experiments were performed in a shielded black box using an usual three electrode configuration. The working electrode of p-SiC on Si substrate had an effective surface area of 0.5 cm^2. The counter electrode and the reference electrode were a Pt loop and Ag/AgCl electrode in 3 M NaCl solution, respectively. Illumination source used for PEC experiments was a Zahner LED with different wavelengths at a constant intensity of 100 W m^{-2}. The electrolyte solution used was 0.1 M H_2SO_4 and the pH is 0.8 measured by pH meter.

A scanning potentiostat was used for the measurement of current–potential dependence and IPCE curves. Mass spectrometry (MS) was used to detect the generated gas in the PEC cell.

3. Results and discussion

3.1. p-Type 3C-SiC film on p-Si substrate used as a photoelectrode in PEC cell

Photoresponse measurements were carried out by means of a potentiostat in a three-electrode setup with Ag/AgCl as the reference electrode and Pt as the counter electrode. A potential scan was started from the cathodic region toward the anodic region with chopped light. The scanning rate was 20 mV s^{-1}. The dependence of photocurrent density on potential with the p-SiC film on p-Si substrate under chopped light illumination is shown in Fig. 1. In the course of the cathodic scan the cathodic photocurrent shows a continuous increase with increasing the external negative bias, indicating an appreciable photocurrent generation at the photoelectrode, which corresponds to hydrogen evolution at the surface of the p-SiC films on p-Si substrate and at the same time oxygen evolution on Pt electrode. However, in the course of the anodic scan an anodic photocurrent is also generated. The anodic photocurrent increases with increasing the external positive bias (see the inlet curve in Fig. 1), indicating the film exhibits an anodic photocurrent behavior as a photoanode. The appearance of the photocurrent indicates that the corresponding anodic bias on the electrode of the p-SiC film on p-Si substrate leads to light induced holes transfer to the electrolytic solution. Therefore, the PEC measurements indicates the p-SiC film on p-Si substrate can generate a cathodic photocurrent as a photocathode, which mostly corresponds to hydrogen production, and generate an anodic photocurrent as a photoanode, which mostly corresponds to oxygen evolution. This is a quite interesting phenomenon. From the literature on the topic of water splitting we found few analysis on this phenomenon. For p-type films all the researchers just focus on the cathodic scan for generating photocurrent in PEC experiments [17–22,25]. We will concentrate on this novel anodic photocurrent behavior of the p-SiC film on p-Si in the following part.

Fig. 2 shows current density–potential curves of the p-SiC film on p-Si substrate under light illumination with different

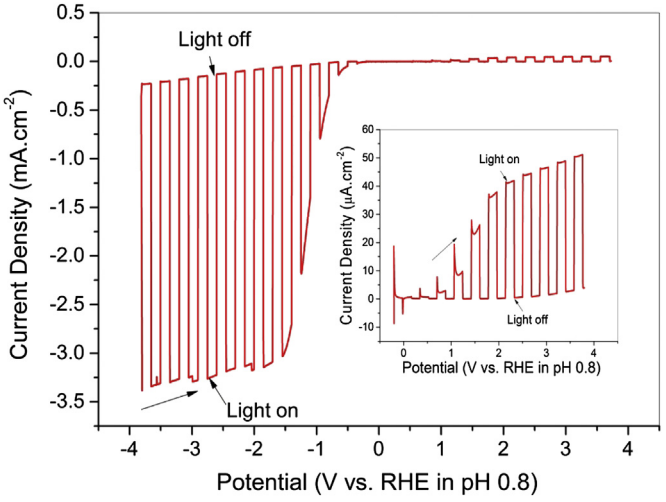

Fig. 1. Current density–potential curves of the p-SiC film on p-Si substrate under chopped light illumination. The light intensity was set at 100 W m^{-2}.

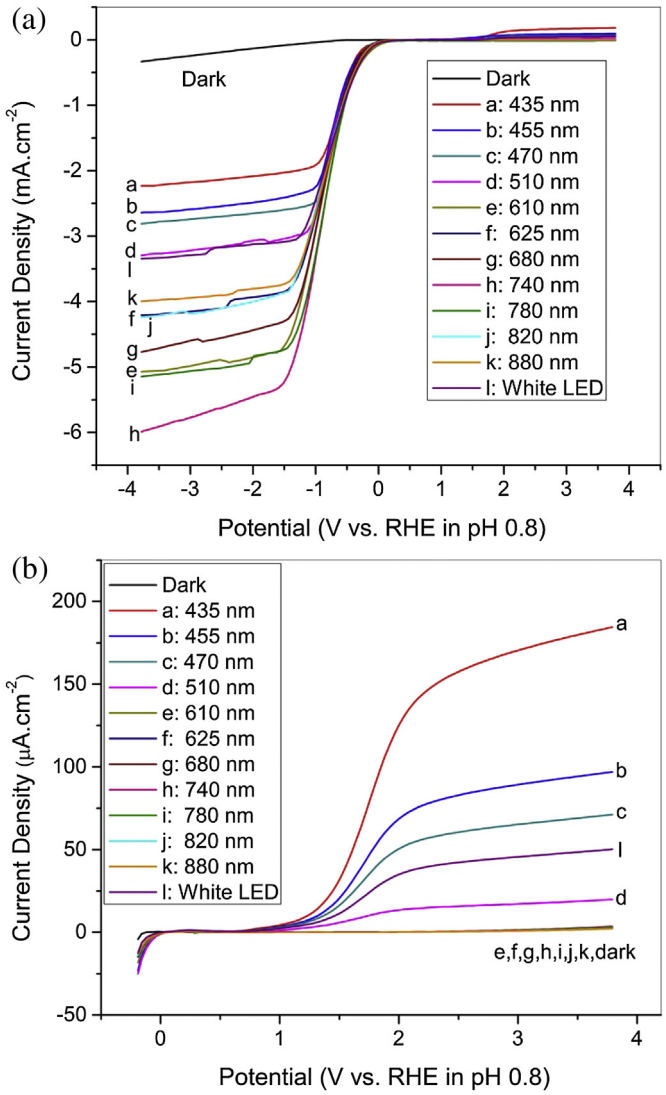

Fig. 2. Current density–potential curves of the p-SiC film on p-Si substrate under light illumination with different wavelengths. (a) potential: −3.6 to 4.0 V; (b) potential: 0–4.0 V. The light intensity was set at 100 W m^{-2}.

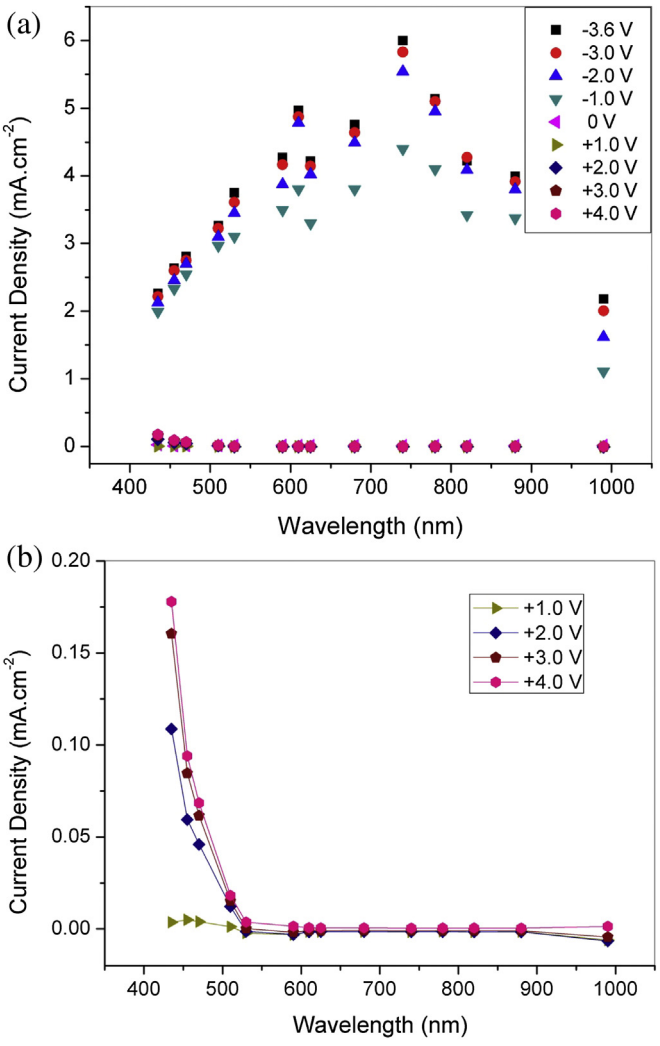

Fig. 3. Variations of Current density on wavelength at different potentials.

wavelengths from 435 to 880 nm. The light intensity for all the light sources was set at 100 W m^{-2}. It shows that the p-SiC film on p-Si as the cathode can generate cathodic photocurrents under illumination by all the light sources with different wavelengths. The film can get a highest cathodic photocurrent density with the light wavelength of 740 nm as the illumination source. However, when it acts as the photoanode, the anodic photocurrent decreases with increasing the wavelength, see Fig. 2(b). But beyond 510 nm it almost cannot generate the photocurrent. The variations of current density on wavelength at different potentials are shown in Fig. 3. From Fig. 3, it is clearly seen that there are two photocurrent peaks on the curves with the external negative bias: one is at 610 nm and the other one is at 740 nm. The 3C-SiC bandgap is around 2.3 eV so it can absorb the light below 530 nm. The Si bandgap is 1.1 eV, which can absorb the light till the wavelength of 1100 nm. For water splitting, it request the bandgap of the semiconductor should be at least 1.23 eV in theory. But considering the overpotential on the electrode, the minimum bandgap would be in the range of 1.6–1.9 eV, accordingly which also can absorb the light with the wavelength in the range of 650–775 nm. So the highest cathodic photocurrent at a wavelength of 740 nm would be achieved from the contribution of Si. However, these multiple peaks may also be attributed to the LED intensities, which need to be studied further later. But with the external positive bias the p-SiC film on p-Si as a photoanode can only generate anodic photocurrents below 550 nm, see Fig. 3(b).

In order to address the quantitative correlation between photocurrent and light absorption of the p-SiC film on p-Si, we performed incident-photon-to-current-conversion efficiency (IPCE) measurements to study the photoactive wavelength regimes for the p-SiC film on p-Si and the p-Si (Fig. 4). IPCE can be expressed as [29]

$$\mathrm{IPCE} = (1240 \times I)/\left(\lambda \times J_{\mathrm{light}}\right)$$

where I is the photocurrent density, λ the incident light wavelength, and J_{light} the measured irradiance. IPCE curves measured at different potentials for the p-SiC film on p-Si and the p-Si are show in Fig. 4. The precipitous drop in IPCE at 725 nm was caused by the recording delay of the system. It can be observed that the p-SiC film on p-Si with an external negative bias presents a little higher IPCE value in the visible region in relation to p-Si. The IPCE of the p-SiC on p-Si and the p-Si as photocathodes in the visible region are 80%

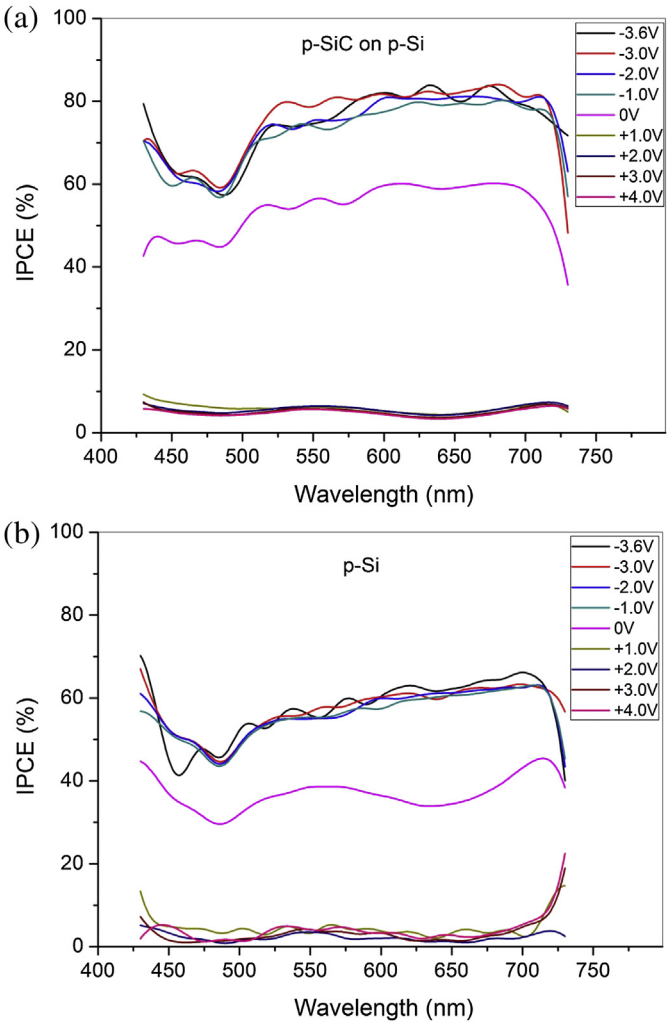

Fig. 4. IPCE curves measured at different potentials: (a) p-SiC film on p-Si; (b) p-Si.

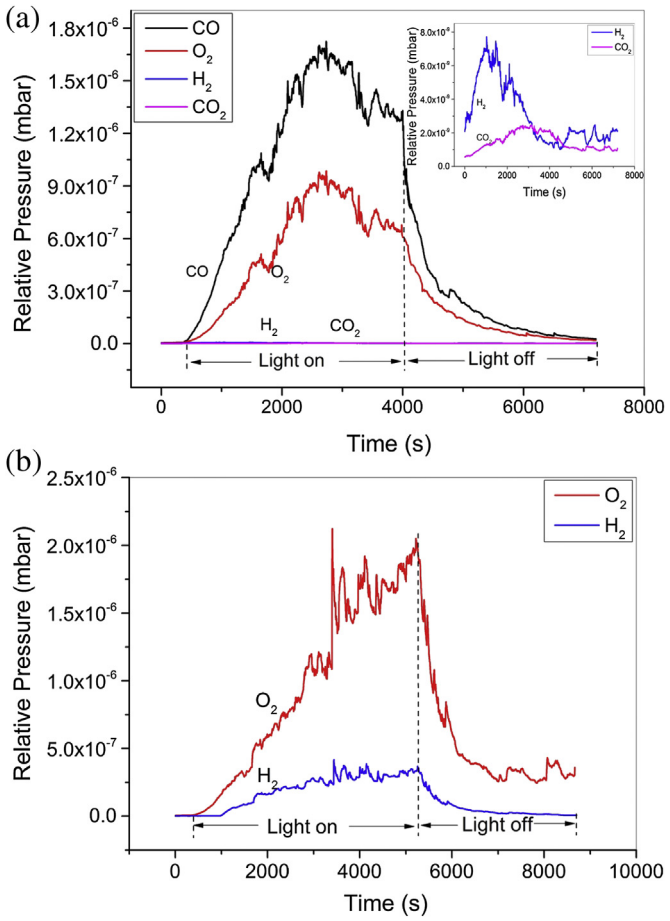

Fig. 5. Mass spectra of p-SiC on p-Si for gas generation in PEC cell: (a) photoanode; (b) photocathode.

and 60%, respectively, which confirms that SiC film can contribute to the photocurrent under light illumination. These results clearly suggest that the (e^-)–(h^+) recombination process on the electrode surface is very low, which is helpful for water splitting. However, both present a very low IPCE value when acting as photoanodes. So from Fig. 4(a) and (b), it demonstrates that the measured cathodic photocurrents with the structure p-SiC film on p-Si are generated by the p-SiC and the p-Si together under light illumination.

The gas generation tests of p-SiC on p-Si as the photoanode under anodic bias and as the photocathode under cathodic bias were performed in the PEC system with MS. The mass spectra are showed in Fig. 5. From the mass spectrum in Fig. 5(a) it indicates that p-SiC on p-Si as the photoanode can generate O_2 while CO was formed due to the surface oxidation but less CO_2 detected by MS. With the PEC test going on, the photocurrent was decreased due to the surface oxidation, which resulted in H_2 generation rate decreased. Besides, due to the small current (tens of micro-Amps) the generated small H_2 bubbles were attached on the counter electrode (Pt wire loop). Most of small H_2 bubbles could not move to the top of the PEC cell except for a few big bubbles. According to the mass spectrum, it can be concluded that the small (tens of micro-Amps) of current observed under anodic bias in Figs. 1 and 2 stems from both photocurrent and surface oxidative current. The mass spectrum in Fig. 5(b) shows that our PEC system with the p-SiC on p-Si as the photocathode can split the water into H_2 and O_2 under light illumination. After H_2 generated on the surface of SiC, part of H_2 can be absorbed by SiC electrode as confirmed by van Dorp et al. [30], which caused the low amount of H_2 detected by MS.

As presented in Figs. 1 and 2, the p-type 3C-SiC film on p-type Si substrate shows the anodic photocurrent behavior as the anode and the cathodic photocurrent behavior as the cathode under light illumination. For isotype heterojunction semiconductors such as p-SiC on p-Si, the current–voltage curve is more complicated. In our case, the p-SiC film with the bandgap of 2.3 eV is on the Si substrate with the bandgap of 1.1 eV. Due to different work functions between SiC and Si, the energy bands are bent. For isotype heterojunction semiconductors, the current density is given by [31]

$$J = \frac{q\Psi_{bi}A^*T}{k}\left(1-\frac{V}{\Psi_{bi}}\right)\exp\left(\frac{-q\Psi_{b1}}{kT}\right)\exp\left(\frac{-q\varnothing_b}{kT}\right)\left[\exp\left(\frac{qV}{kT}\right)-1\right] \quad (1)$$

where J is the current density, q the electron charge, A^* the effective Richardson constant, $\varnothing_b$ the barrier height, V applied voltage. The total built-in potential Ψ_{bi} is equal to the sum of partial built-in voltages ($\Psi_{b1} + \Psi_{b2}$), where Ψ_{b1} and Ψ_{b2} are the electrostatic potentials supported at equilibrium by semiconductors 1 and 2, respectively. The reverse current never saturates but increases linearly with voltage at large $-V$. In the forward direction, the dependence of J on V can be approximated by an exponential function $J \propto [\exp(qV/\eta kT)]$ where the ideality factor η generally has a value between 1 (for diffusion current) and 2 (for recombination

current). When a negative bias is applied to the counter electrode, the SiC film gets the negative voltage by considering the electrolyte as the conductive wire and vice versa. Due to the open-circuit potential in the electrolyte, the current "0" point in Equation (1) is shifted compared with the *I*–*V* curve of hetero p–p structure diode measured in air. From Figs. 1 and 2, the electrode p-SiC film on p-Si in PEC cell can generate the obvious photocurrent in the reverse current region and the weak photocurrent in the forward current region after being illuminated by light. It indicates a heterojunction semiconductor can generate a cathodic photocurrent as a cathode and an anodic photocurrent as an anode [32]. For the p-SiC film on p-Si with light illumination in the reverse current region, the electrode as the cathode creates electrons and holes. The minority electrons reduce protons or water at the electrode to produce hydrogen. In the forward current region most of the created electrons and holes can be easily recombined and the photocurrent is only contributed from the SiC as confirmed from IPCE curves in Fig. 4 so that the photocurrent is much lower compared with the cathodic photocurrent. But by applying the higher bias some holes can be moved to electrode surface from the SiC for oxidizing water to oxygen, which makes the onset potential shifted to the positive direction.

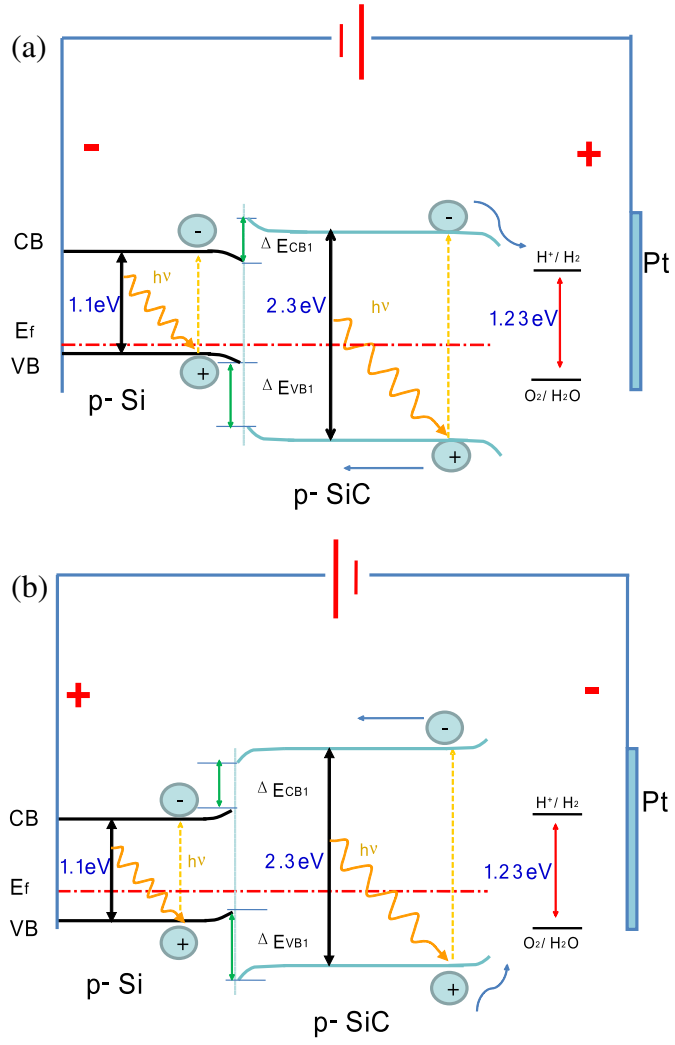

Fig. 6. Energy diagrams of PEC components: photocathode (p-SiC on p-Si), anode (Pt) and light illumination: (a) with an external negative bias and (b) with an external positive bias.

The photocurrent–potential curve can be explained by energy diagrams, see Fig. 6. As the SiC absorbs one photon, it can generate one pair of electron and hole, the same as the Si substrate. After the external negative bias is applied to the electrode, the electron from SiC will be driven to the hydrogen redox potential and produce hydrogen. Since the barrier of conduction bands between p-SiC and p-Si is very small, a few photogenerated electrons from the Si substrate can jump into the SiC with a higher external negative bias due to tunneling effect and then some electrons can move to the SiC surface for hydrogen evolution before recombination, which contributes to increase the cathodic photocurrent. But when it acts as the photoanode, the holes generated from the SiC can be driven to the oxygen redox potential before recombination and produce oxygen by applying the higher external positive bias. But the holes generated from the Si cannot be driven into SiC due to the large barrier of valence bands between p-SiC and p-Si. Hence, the anodic photocurrent is quite small with the contribution only from the SiC. Moreover, for oxygen evolution the generated holes from SiC need more external energy to move to the oxygen redox potential due to the rapid recombination of holes and electrons, which results in the anodic cut-off potential shifted more to the positive axis direction far away from "0" point compared with the onset cathodic cut-off potential as shown in Figs. 1 and 2. Therefore, the p-SiC film on p-Si substrate can generate a strong cathodic photocurrent as a photocathode, and generate a weak anodic photocurrent as a photoanode. As is known, for a single p-type semiconductor as the typical diode, the reverse current saturates below the negative breakdown voltage but the current increase rapidly in the forward direction. When the single p-type semiconductor is used as a photoelectrode in PEC cell, it can generate an apparent cathodic photocurrent in the reverse current region [33]. But for the p-type 3C-SiC film on p-Si substrate it is not one single layer but two hetero-layers so that it can generate a strong cathodic photocurrent as a photocathode, which corresponds to hydrogen production, and generate a weak anodic photocurrent as a photoanode, which corresponds to oxygen evolution, as shown in Figs. 1 and 2.

3.2. *p-Type 3C-SiC film on n-Si substrate used as a photoelectrode in PEC cell*

Fig. 7 shows the current density–potential curves of the p-SiC film on n-Si substrate in dark and under light illumination in the PEC cell. No apparent photocurrent is observed in the range of

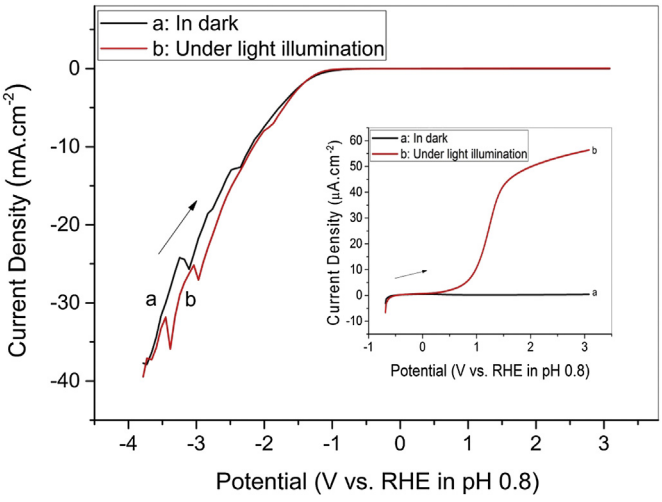

Fig. 7. Current density–potential curves of the p-SiC film on n-Si substrate in dark and under light illumination.

negative potential from −3.6 to 0 V although very weak photocurrent exists, indicating the p-SiC film on n-Si cannot generate an obvious cathodic photocurrent as the photocathode. But in the positive region of bias it shows an appreciable photocurrent generation under light illumination compared with the current density–potential curve in dark. In this case the p-SiC film on n-Si substrate can be used as an anode for oxygen evolution, which shows an anodic photocurrent behavior for water splitting. So such kind of structure is also very interesting to solar oxygen evolution.

For anisotype heterojunction semiconductors, the diffusion currents are similar to a regular p–n junction. So the total current is decided by electron and hole diffusion current and given by [31]

$$J = J_n + J_p = \left(\frac{qD_{n2}n_{i2}^2}{L_{n2}N_{A2}} + \frac{qD_{p1}n_{i1}^2}{L_{p1}N_{D1}}\right)\left[\exp\left(\frac{qV}{kT}\right) - 1\right] \quad (2)$$

where J is the current density, J_n the electron diffusion current, J_p the hole diffusion current, q the electron charge, V applied voltage, T the temperature.

$$J_0 = \left(\frac{qD_{n2}n_{i2}^2}{L_{n2}N_{A2}} + \frac{qD_{p1}n_{i1}^2}{L_{p1}N_{D1}}\right) \quad (3)$$

In the reverse direction the current density saturates at $-J_0$ and in the forward direction the current will rapidly increase approximately as exp (qV/kT). As discussed above the semiconductor electrode can generate an appreciable photocurrent in the reverse current region. It indicates that the p-SiC film on n-Si can generate an obvious anodic photocurrent as a photoanode. The photocurrent behavior of the p-SiC on n-Si can also be explained by energy diagrams, see Fig. 8. When p-SiC absorbs one photon, it can generate one pair of electron and hole, the same as the n-Si substrate. With an external negative bias applied to the electrode, the electrons from the SiC surface can move to the hydrogen redox potential for hydrogen evolution. However, for the photogenerated electrons in Si, it is almost not possible to jump into SiC due to the large barrier between conduction bands. In the forward current region the dark current is very large by itself so that the weak cathodic photocurrent is not obvious on the current–potential curve although it exists indeed as shown in Fig. 7. When the external positive bias is applied to the electrode, the photogenerated holes from SiC can be driven to oxidize the water. A few photogenerated holes from Si would also contribute the anodic photocurrent due to tunneling effect. Although the anodic photocurrent is not comparable due to the fast recombination and the low IPCE, the p-SiC film on n-Si can be used as an anode for solar water splitting.

4. Conclusion

The electrochemical properties of single-crystalline p-type 3C-SiC films on p-Si and n-Si substrates were investigated as electrodes in H_2SO_4 aqueous solutions in dark and under light illumination. The PEC measurements indicates the p-SiC film on p-Si substrate can generate the cathodic photocurrent as the photocathode, which corresponds to hydrogen production, and generate the anodic photocurrent as the photoanode, which corresponds to oxygen evolution. The p-SiC film on p-Si as the cathode can get the highest cathodic photocurrent density with the light wavelength of 740 nm as the illumination source. But acting as the photoanode its anodic photocurrent decreases with increasing the wavelength. Beyond 510 nm it almost cannot generate the photocurrent as the photoanode. The IPCE of the p-SiC on p-Si and the p-Si as the photocathode in the visible region are 80% and 60%, respectively but both present a very low IPCE value as the photoanode. The mass spectra

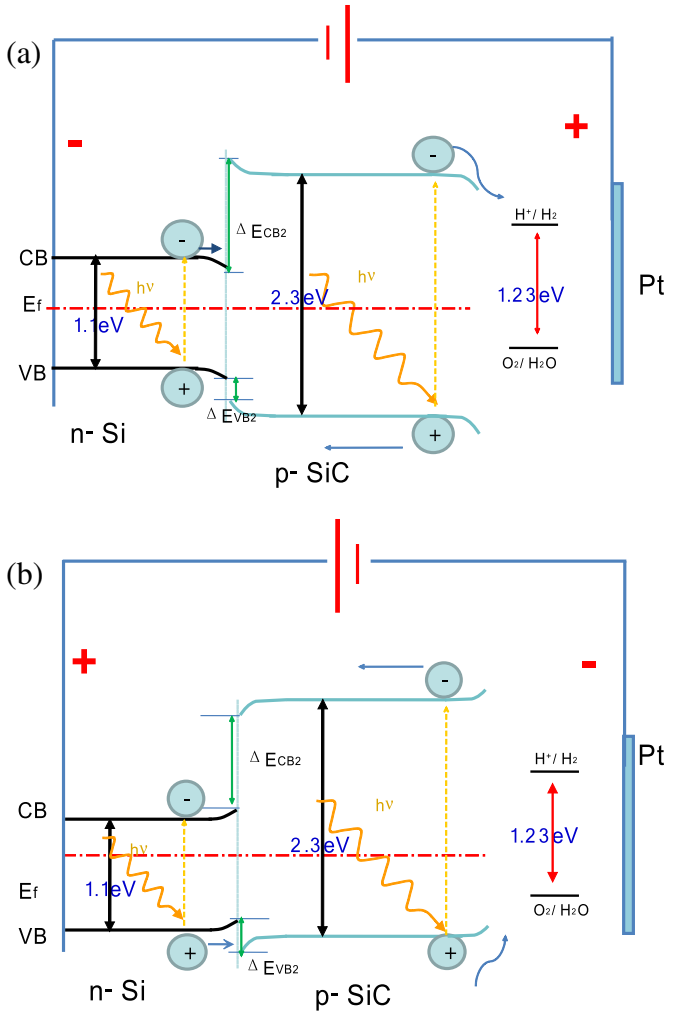

Fig. 8. Energy diagrams of PEC components: photocathode (p-SiC on n-Si), anode (Pt) and light illumination: (a) with an external negative bias and (b) with an external positive bias.

confirm that p-SiC on p-Si as the photoanode can generate O_2 while CO was formed due to the surface oxidation but less CO_2 detected while as the photoanode it can split the water into H_2 and O_2 under light illumination. For p-type 3C-SiC film on n-Si substrate, it can generate an appreciable anodic photocurrent as the photoanode for oxygen evolution.

Acknowledgments

The authors gratefully acknowledge the financial support of this work by the BMBF Foundation of Germany, project "H_2Nanosolar" No. 03SF0353E, and the authors also acknowledge the donation of single-crystalline 3C-SiC samples by the Leibniz Institute for Crystal Growth, Berlin, Germany, Mr. Ad Wonders for the assistance and discussion of mass spectrum at Eindhoven University of Technology, the Netherlands, and our colleagues Mr. Jürgen Ziegler, Mr. Dominic Fertig, Dr. Wolfram Calvet and Mr. Eswaran Murugasen, etc for their supports during the experiments.

References

[1] M. Momirlan, T.N. Veziroglu, Sustain. Energy Rev. 6 (2002) 141–179.
[2] A. Fujishima, K. Honda, Nature 238 (1972) 37–38.
[3] T. Hisatomi, K. Domen, Proc. SPIE 7408 (2009) 740802.

[4] N.S. Lewis, J. Electroanal. Chem. 508 (2001) 1–10.
[5] H. Tributsch, Int. J. Hydrogen Energy 33 (2008) 5911–5930.
[6] R.N. Pandey, K.S. Chandra Babu, N. Srivastava, Prog. Surf. Sci. 52 (1996) 125–192.
[7] E. Serrano, G. Rus, J. Garcia-Martinez, Renew. Sustain. Energy Rev. 13 (2009) 2373–2384.
[8] M. Momirlan, T. Veziroglu, Renew. Sustain. Energy Rev. 3 (1999) 219–231.
[9] M. Ashokku, Int. J. Hydrogen Energy 23 (1998) 427–438.
[10] S.S. Penner, Energy 31 (2006) 33–43.
[11] J. Nowotny, C.C. Sorrell, L.R. Sheppard, T. Bak, Int. J. Hydrogen Energy 30 (2005) 521–544.
[12] A. Currao, Chimia 61 (2007) 815–819.
[13] K. Rajeshwar, P. Singh, J. Dubow, Electrochim. Acta 23 (1978) 1117–1144.
[14] R. Memming, Electrochim. Acta 25 (1980) 77–88.
[15] H. Wang, T. Deutsch, J.A. Turner, ECS Trans. 6 (2008) 37–44.
[16] H. Wang, T. Deutsch, J.A. Turner, J. Electrochem. Soc. 155 (2008) F91–F96.
[17] O. Khaselev, J.A. Turne, J. Electrochem. Soc. 145 (1998) 3335–3339.
[18] H. Wang, J.A. Turner, ECS Trans. 27 (2007) 125–133.
[19] J.N. Nian, C.C. Hu, H. Teng, Int. J. Hydrogen Energy 33 (2008) 2897–2903.
[20] C.-C. Hu, J.N. Nian, H. Teng, Sol. Energy Mater. Sol. C 92 (2008) 1071–1076.
[21] S. Somasundaram, C.R.N. Chenthamarakshan, N.R. de Tacconi, K. Rajeshwar, Int. J. Hydrogen Energy 32 (2007) 4661–4669.
[22] R.M. Liang, Y.M. Chang, P.W. Wu, P. Lin, Thin Solid Films 518 (2010) 7191–7195.
[23] K. Aryal, B.N. Pantha, J. Li, J.Y. Lin, H.X. Jiang, Appl. Phys. Lett. 96 (2010) 052110.
[24] J. Li, J.Y. Lin, H.X. Jiang, Appl. Phys. Lett. 93 (2008) 162107.
[25] W.B. Ingler Jr., S.U.M. Khan, Int. J. Hydrogen Energy 30 (2005) 821–827.
[26] I. Lauermann, R. Memming, D. Meissner, J. Electroanal. Chem. 144 (1997) 73–80.
[27] P.J. Sebastian, N.R. Mathews, X. Mathew, M. Pattabi, J. Turner, Int. J. Hydrogen Energy 26 (2001) 123–125.
[28] J. Akikusa, S.U.M. Khan, Int. J. Hydrogen Energy 27 (2002) 863–870.
[29] X. Yang, A. Wolcott, G. Wang, A. Sobo, R. Carl Fitzmorris, F. Qian, J.Z. Zhang, Y. Li, Nano Lett. 9 (2009) 2331–2336.
[30] D.H. van Dorp, N. Hijnen, M.D. Vece, J.J. Kelly, Angew. Chem. Int. Ed. 48 (2009) 6085–6088.
[31] S.M. Sze, K.K. Ng, Physics of Semiconductor Devices, third ed., Physical Electronics, Inc, New York, Wiley, 2007.
[32] Q.B. Ma, B. Kaiser, J. Ziegler, D. Fertig, W. Jaegermann, J. Phys. D Appl. Phys. 45 (2012) 325101.
[33] B. Kaiser, D. Fertig, J. Ziegler, J. Klett, S. Hoch, W. Jaegermann, ChemPhysChem 13 (2012) 3053–3060.